ELSEVIER

Journal of Structural Geology 29 (2007) 1114–1130

JOURNAL OF STRUCTURAL GEOLOGY

www.elsevier.com/locate/jsg

Slow and fast deformation in the Dora Maira Massif, Italian Alps: Pseudotachylytes and inferences on exhumation history

M.S. Zechmeister [a], E.C. Ferré [b,*], M.A. Cosca [c], J.W. Geissman [d]

[a] *Department of Geology and Geophysics, The University of Oklahoma, Norman, OK 73019, USA*
[b] *School of Geology, Southern Illinois University, Carbondale, IL 62901, USA*
[c] *Institute of Mineralogy and Geochemistry, University of Lausanne, CH-1015 Lausanne, Switzerland*
[d] *Department of Earth and Planetary Sciences, University of New Mexico, Albuquerque, NM 87131-1116, USA*

Received 20 October 2006; received in revised form 16 February 2007; accepted 4 March 2007
Available online 16 March 2007

Abstract

The Dora Maira Massif (DM), Western Alps is a type example of an ultra-high pressure (UHP) metamorphic terrain. The occurrence of pseudotachylytes within the Val Gilba area of DM led to speculation regarding the role of seismic slip in the exhumation of the massif. In this study, new field, microstructural and geochemical data on the pseudotachylyte veins and their mylonitic gneiss host are presented. The formation of pseudotachylyte veins occurred late in the exhumation history at 20.1 ± 0.5 Ma and at shallow depths (<3 km), long after the early stages and rapid exhumation that is characteristic of UHP massifs. Preseismic, coseismic and postseismic deformation features suggest that seismic slip occurred at a period where the geologic strain rate was particularly low. This observation is explained by a stick-slip model along the mylonitic foliation plane in which slip was preferentially along phengite-chlorite rich layers. Frictional sliding instability is promoted by a slow slip rate, by a phenomenon similar to ''brake shuttering'' in automobiles. An alternative explanation could be provided by climatically driven, accelerated exhumation ca. 20 Ma, as suggested by the 20 Ma-old white micas reported in the Tertiary Piedmont Basin.

Keywords: Pseudotachylyte; Exhumation; UHP; Brittle deformation

1. Introduction

The evolution of orogenic belts results from the integration of deformation at all time scales. Yet, the relationship between slow deformation, which typically takes place at low strain rates ($\approx 10^{-14}$ to 10^{-15} s^{-1}), and fast deformation, which takes place at faster rates ($\approx 10^{\circ}$ to 10^{-2} s^{-1}), is not well understood. Fault-related pseudotachylytes are commonly found in orogenic domains. These rocks require seismic deformation rates to form by frictional melting (e.g., McKenzie and Brune, 1972; Sibson, 1975). Hence, these ''fossils'' of ancient earthquakes (Lin, 1994; Cowan, 1999; Andersen and Austrheim, 2006) might provide valuable insights into seismic deformation processes.

The Western Alps are a young and active orogenic belt that hosts several pseudotachylyte occurrences in various rock types (e.g., Masch, 1970; Henry, 1990; Koch and Masch, 1992; Techmer et al., 1992; Obata and Karato, 1995; Di Toro and Pennacchioni, 2004, 2005). One of these localities, the Dora Maira Massif, is an example of an ultra-high pressure (UHP) metamorphic province. This massif is characterized by fast exhumation rates following the peak of UHP metamorphism around 35–30 Ma (Gebauer et al., 1997; Di Vincenzo et al., 2006). The pseudotachylyte generation veins in the Dora Maira Massif are remarkably planar and conformable with a low-angle mylonitic foliation that formed during exhumation, under greenschist facies conditions (Henry, 1990). This control on the vein geometry exerted by the host rock

* Corresponding author.
E-mail address: eferre@geo.siu.edu (E.C. Ferré).

0191-8141/$ - see front matter © 2007 Elsevier Ltd. All rights reserved.
doi:10.1016/j.jsg.2007.03.009

preseismic fabric, also observed in other localities (Magloughlin, 1989; Wenk et al., 2000), provides opportunities to understand better the link between slow and fast deformation. Pseudotachylyte injection veins and networks (Ferré et al., 2005) are less common than generation veins.

The occurrence of fault-related pseudotachylyte veins is common in UHP units (e.g., Webb et al., 2001; Lin et al., 2003; Lund and Austrheim, 2003) and this might be related to the fast exhumation rates that characterize these massifs. In addition, pre-existing strength anisotropies in the host gneiss might contribute to extreme plastic then cataclastic strain localization. At variance with Hobbs et al. (1986) stick-slip model, recent modeling suggests that in a homogeneous medium, strain localization during ductile deformation does not normally occur unless there is an external perturbation to the system (Montési and Hirth, 2003). One external cause that could account for abrupt changes in deformation rate would be a climatically driven, accelerated erosion that, in turn, would lead to faster unroofing of the Dora Maira UHP units.

In order to investigate these questions, detailed observations were carried out in the Dora Maira Massif. New field and microstructural data on these veins are presented with evidence for frictional melting and inferences on the massif exhumation history are discussed.

2. Geologic setting of the Dora Maira Massif

2.1. The Alpine Internal Zones

The Western Alps are characterized by kilometer scale E-W trending sheath folds, with northwest vergence, and Internal Crystalline Massifs such as the Monte Rosa Massif (Lacassin and Mattauer, 1985). These ductile alpine structures formed during retrograde metamorphism contemporaneous with exhumation. Ductile strain localization led to formation of mylonites with a consistent top-to-west sense of shear. Mineral and stretching lineations consistently trend E-W throughout the Internal Crystalline Massifs and formed during greenschist facies retrograde metamorphism (Wheeler, 1991; Avigad et al., 2003 and references therein).

In contrast, the Piedmont-Ligurian units and the Briançonnais Zone, to the west of the studied area (Fig. 1), exhibit consistent top-to-east sense of shear (Philippot, 1990; Caby, 1996; Caby and Ricou, 1999; Agard et al., 2002). This plastic deformation event is well recorded in carpholite-lawsonite, blueschist and garnet-blueschist assemblages in ocean-derived units.

2.2. Tectono-metamorphic evolution of the Dora Maira Massif

The discovery of coesite in the Dora Maira Massif led to considerable reconsideration of the fate of continental crust during collision (Chopin, 1984). Indeed, the presence of this silica polymorph requires pressures of at least 2.8 GPa consistent with subduction of these crustal rocks to great depths (>100 km; Hacker and Peacock, 1994). The Dora Maira Massif (Fig. 1) has been extensively studied (e.g., Wheeler, 1991; Avigad, 1992; Henry et al., 1993; Michard et al., 1993; Gebauer et al., 1997; Compagnoni and Hirajima, 2001; Avigad et al., 2003; Hermann, 2003) and has become a classic locality for UHP continental crust metamorphism. This dome-shaped massif (Fig. 2) represents a window of pre-Alpine continental crust overlain by relics of a Mesozoic sedimentary cover. The cover itself is capped by ocean-derived Piemont-Ligurian units that have undergone eclogite facies metamorphism.

Chloritoid-talc-garnet assemblages in metapelites and zoisite-omphacite-garnet assemblages in mafic eclogites are common in most parts of the Dora Maira Massif. Chloritoid-talc-kyanite-pyrope-coesite (UHP) assemblages are particularly well exposed in our study area (Chopin et al., 1991). These coesite-bearing rocks form a slice $\approx$1 km exposed towards the base of the tectonic pile. The metamorphic conditions determined for these assemblages indicate peak pressure of 3.0–3.4 GPa (Schertl et al., 1991; Sharp et al., 1993), and even as high as 4.2 GPa (i.e., $\approx$150 km; Chopin and Schertl, 1999), with peak temperatures around 800 °C. The paleogeothermal gradient of 6–8 °C km^{-1}, deduced from these values, is characteristic of subduction settings.

The coesite-bearing UHP unit overlies lower greenschist facies metasediments and igneous rocks of the Sanfront-Pinerolo unit (Figs. 1 and 2) that never experienced pressures exceeding 0.75 GPa with maximum temperatures of about 550 °C (Avigad et al., 2003). Thus, the major tectonic contact at the base of the UHP coesite unit documents a pressure gap $\geq$2.5 GPa. An orthogneiss unit, exposed on top of the UHP coesite unit, displays assemblages indicative of a pervasive greenschist facies overprint and lack of HP assemblages. The orthogneiss unit underlies mafic eclogites, derived from Mesozoic gabbros, and from which pressures of 2.4 GPa and temperatures of 600 °C have been calculated (Messiga et al., 1999).

The early exhumation of the coesite unit, from depths as great as 150 km, is characterized by ductile, non-coaxial strain recorded in coesite-bearing gneisses (Henry, 1990). Deformation became increasingly localized as shown by the formation of syn-kinematic mylonites under greenschist facies metamorphic conditions (Henry et al., 1993). The later stages of exhumation are marked by further partition of deformation in narrow bands of ultramylonite-ultracataclasite-pseudotachylyte that are sub-parallel to the mylonitic foliation (Henry, 1990, p. 130; Cosca et al., 2005). The progressively localized nature of this deformation into increasingly narrower domains suggests that the formation of pseudotachylyte veins results from the same kinematic continuum as the ductile deformation.

The Dora Maira pseudotachylyte veins most likely formed as a result of seismic slip, which is a thermodynamic requirement for their formation (e.g., McKenzie and Brune, 1972; Sibson, 1975). However, these veins surprisingly do not seem to be associated with any of the major exhumation-related faults that bound the UHP units (Henry, 1990; Fig. 1).

2.3. Kinematics of the Dora Maira Massif

An early mineral lineation, marked by phengite, zoisite and kyanite in weakly to non-retrogressed whiteschists, is

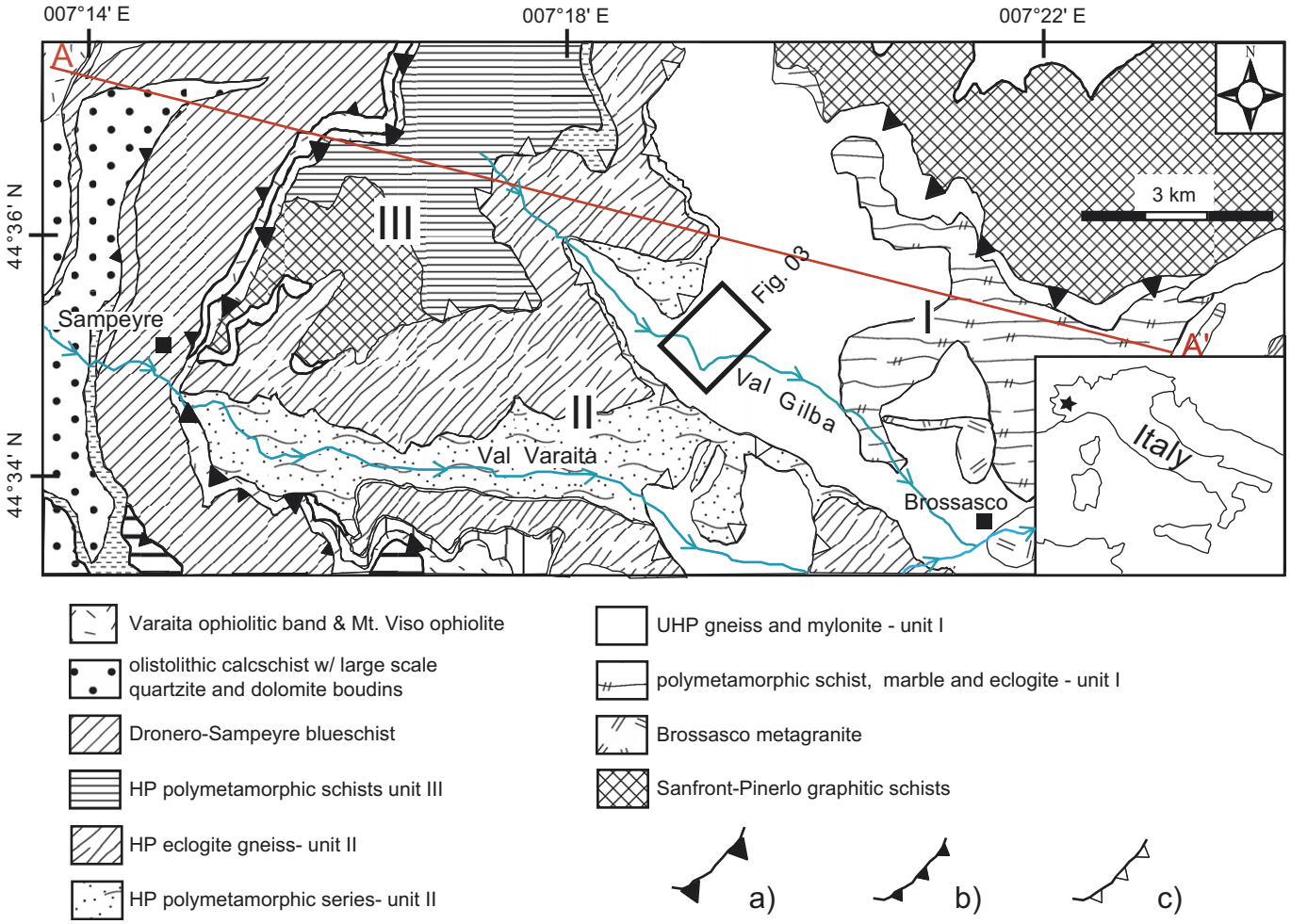

Fig. 1. Geological map of the Val Gilba area in the Dora Maira Massif, Western Alps (modified after Henry et al., 1993 and Avigad et al., 2003). The AA′ cross section is shown on Fig. 2.

preserved but only in a few localities (Philippot, 1990). Evidence of prograde deformation is found in garnet cores such as those of the Case Ramello (Parigi) coarse-grained pyrope-whiteschists. Kinked phengite and undulose quartz grains record syn-exhumation deformation that postdates the peak of metamorphism. The persistence of coronitic microstructures, for example in the center of the Brosasco granite body that is almost undeformed, shows that certain units were somewhat sheltered from retrograde deformation (Bruno et al., 2001). The early fabrics are, however, almost pervasively overprinted by east-west trending mineral lineations and stretching lineations that formed during exhumation.

A significant part of the Dora Maira Massif consists of a medium to fine grained granitic to granodioritic gneiss grading into protomylonites. This unit, the primary host of the pseudotachylyte veins, shows a consistent west-dipping foliation, marked by green biotite, and a consistent EW trending stretching lineation marked by stretched phengite and biotite clasts. High-pressure mineral assemblages, such as garnet, zoisite, phengite and rutile are present as clasts in these strongly deformed orthogneisses. Plagioclase and globular quartz phenocrysts occur in small quartz-dioritic enclaves of unknown origin (aspect ratio L/w $\approx$10:1). These phenocrysts are slightly elongated and exhibit asymmetric tails filled with brown-green biotite. The regional west-dipping green biotite foliation has been interpreted by some authors as the result of regional extension (e.g., Wheeler, 1991; Avigad, 1992; Avigad et al., 1993, 2003). In contrast, others have proposed that this foliation resulted from syn-collisional exhumation (extrusion) assisted by west-dipping normal faulting (Caby, 1996; Cosca et al., 2005).

In the Val Gilba area, the leucogranitic gneisses are particularly well exposed in several small stone quarries (Fig. 1), near the top of the coesite UHP unit and below the quartz-eclogite unit of Avigad et al. (2003). The sense of shear reported for these gneisses in the literature is not consistent, possibly as a result of a significant flattening component in deformation.

2.4. Timing of HP/UHP tectono-metamorphic evolution of the Dora Maira Massif

The geochronology of the Western Alps has been substantially revised by Gebauer (1999), Amato et al. (1999) and Di Vincenzo (2006) who proposed a younger metamorphic

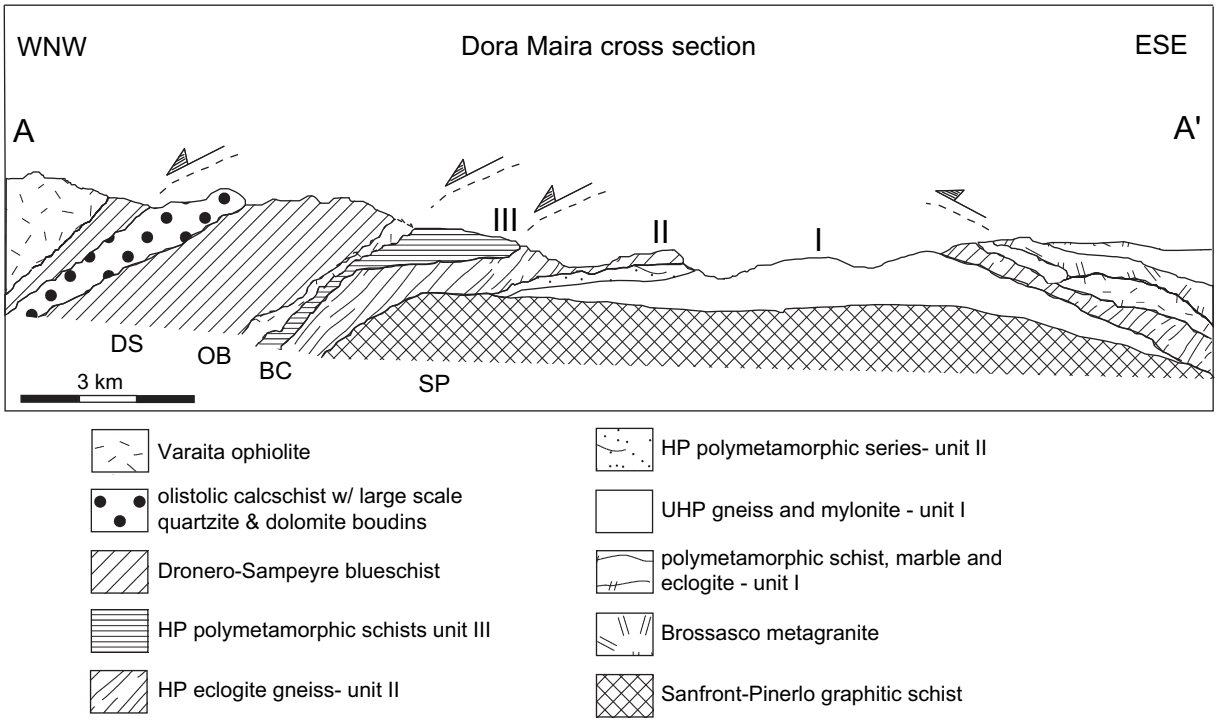

Fig. 2. Cross section in the Val Gilba area in the Dora Maira Massif, Western Alps (simplified after Henry et al., 1993 and Avigad et al., 2003). This cross section is shown on Fig. 1.

evolution than previously thought (e.g., Monié and Philippot, 1989; Cliff et al., 1998). For example, the Zermatt-Saas UHP ophiolite rocks yield a Lu-Hf garnet-omphacite-whole-rock isochron age of 48.8 ± 2.1 Ma at Lago di Cignana (Lapen et al., 2003). Magmatic zircons from the Zermatt coesite eclogite, derived from the Jurassic Piedmont-Ligurian oceanic crust, display metamorphic overgrowths dated by U-Pb at ≈44–45 Ma (Rubatto et al., 1998). The zircons from an eclogite vein in the Monte Viso ophiolite, interpreted as reflecting peak eclogite conditions, yielded an age of 45 ± 1 Ma (Rubatto and Hermann, 2004). In the Dora Maira Massif, metamorphic zircons from the whiteschists of the pyrope-coesite unit are dated by U-Pb SHRIMP at 35.4 ± 1.0 Ma.

Fission track ages indicate that the Dora Maira UHP rocks were already in a near-surface position by ~29.9 Ma (Gebauer et al., 1997). The pseudotachylyte veins, dated at 20.1 ± 0.5 Ma by the $^{40}Ar/^{39}Ar$ method (Cosca et al., 2005), are related to late stages of uplift.

3. New macrostructural data on the Val Gilba gneisses and pseudotachylytes

3.1. Val Gilba augen gneisses and fine to medium grained gneisses

Detailed field observations were conducted in the area within 2 km radius of the Val Gilba stone quarries (Fig. 3; GPS coordinates 44° 35.23′ N, 007° 18.39′ E). The most abundant lithological units consist of two quartzofeldspathic UHP gneiss units defined by Avigad et al. (2003). To the south of the quarries, the main rock type is a fairly homogeneous, mesocratic augen gneiss exhibiting a prominent and consistent protomylonitic to mylonitic foliation (mean 144° 15° W, Fig. 3A). In the quarries and to the north, the main rock type is a leucocratic fine to medium grained gneiss showing a consistent foliation ranging from protomylonitic to ultramylonitic type (Fig. 4A, B and C). The fine to medium grained gneiss is structurally above the augen gneiss. The contact between the two gneisses is parallel to the regional foliation in the study area. The mylonitic foliation consistently strikes NNW-SSE and dips 15–20° to the SW. The mineral lineation trends towards west with a plunge of 10–20° (mean 279° 12°, Fig. 3B). Both types of gneisses consistently display S-C fabrics indicating a top-to-east sense of shear, with an average angle between S- and C- planes of ca. 20° (Fig. 4A). Exposed foliation planes in the augen gneisses reveal substantial asperities due to the presence of large Kfs augens (Fig. 4D).

The fine to medium gneiss is broadly homogeneous even though it locally shows centimeter to meter scale compositional banding parallel to foliation. The banding is defined by varying amounts of phyllosilicates (phengite, biotite, chlorite) and quartz in the gneiss. The phengite-chlorite rich bands display a fine grain size and high strain documented by ribbons of quartz (aspect ratio ≈4:1 to 10:1). Within these bands, phengite clasts have sigmoidal shapes and are surrounded by a rim of biotite. Clusters of biotite, epidote, albite and quartz also form pressure shadows around the phengite clasts. The asymmetry of sigmoidal clasts, pressure shadows and S-C fabrics is consistent with a top-to-west (normal) sense of shear.

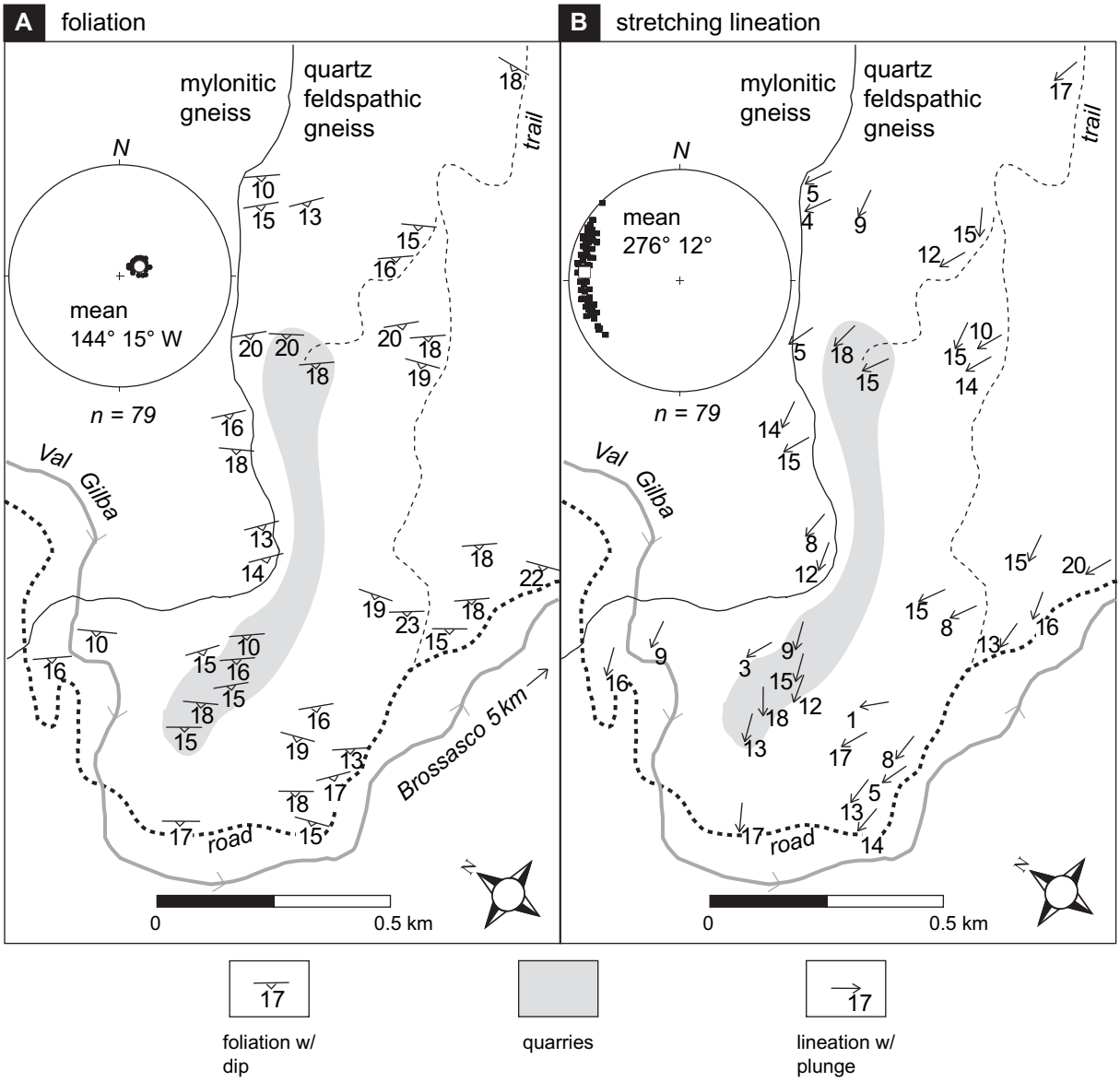

Fig. 3. Structural map of a portion of the Val Gilba area showing location of quarries (exposures of pseudotachylytes). Stereonets are equal area, lower hemisphere. (A) Foliation; (B) stretching lineations.

The average angle between the S and C planes is ca. 30° (Fig. 4B). Compositional banding is also marked by millimeter-thick bands of albite-rich feldspar surrounded by biotite selvages and by millimeter-thick quartz-rich bands adjacent to the phengite-chlorite rich layers. The metamorphic assemblages of biotite replacing phengite clasts and microstructural relationships such as biotite forming pressure shadows around phengite suggests that a substantial part of mylonitic deformation took place at decreasing temperature under epidote amphibolite, greenschist facies conditions.

Ultramylonite deformation (grain size $\leq$50 μm) occurs in narrow phengite-chlorite rich bands (less than a few millimeters thick) that are parallel to the mylonitic foliation. The sense of shear in these ultramylonitic bands, indicated by S-C structures, is top-to-west. These bands are cut at low angles by cataclasite bands and pseudotachylyte veins.

Away from the pseudotachylyte veins, the last increment of macroscopic deformation in the Val Gilba mylonitic gneisses is represented by steep normal faults ($\geq$0.5 km from the quarry) and by vertical gray quartz tension veins, a few centimeters in width, hosting quartz, albite tourmaline and magnetite.

3.2. Val Gilba pseudotachylyte veins and adjacent host rock

The pseudotachylyte veins are commonly hosted by the leucocratic fine to medium grained gneisses in the quarries (Fig. 5) and less commonly hosted by the augen gneisses in a few localities outside the quarries. These veins are common in the fine to medium grained gneisses where they run parallel to the mylonitic foliation over distances up to 100 m. At the outcrop scale, the pseudotachylyte veins do not appear to be

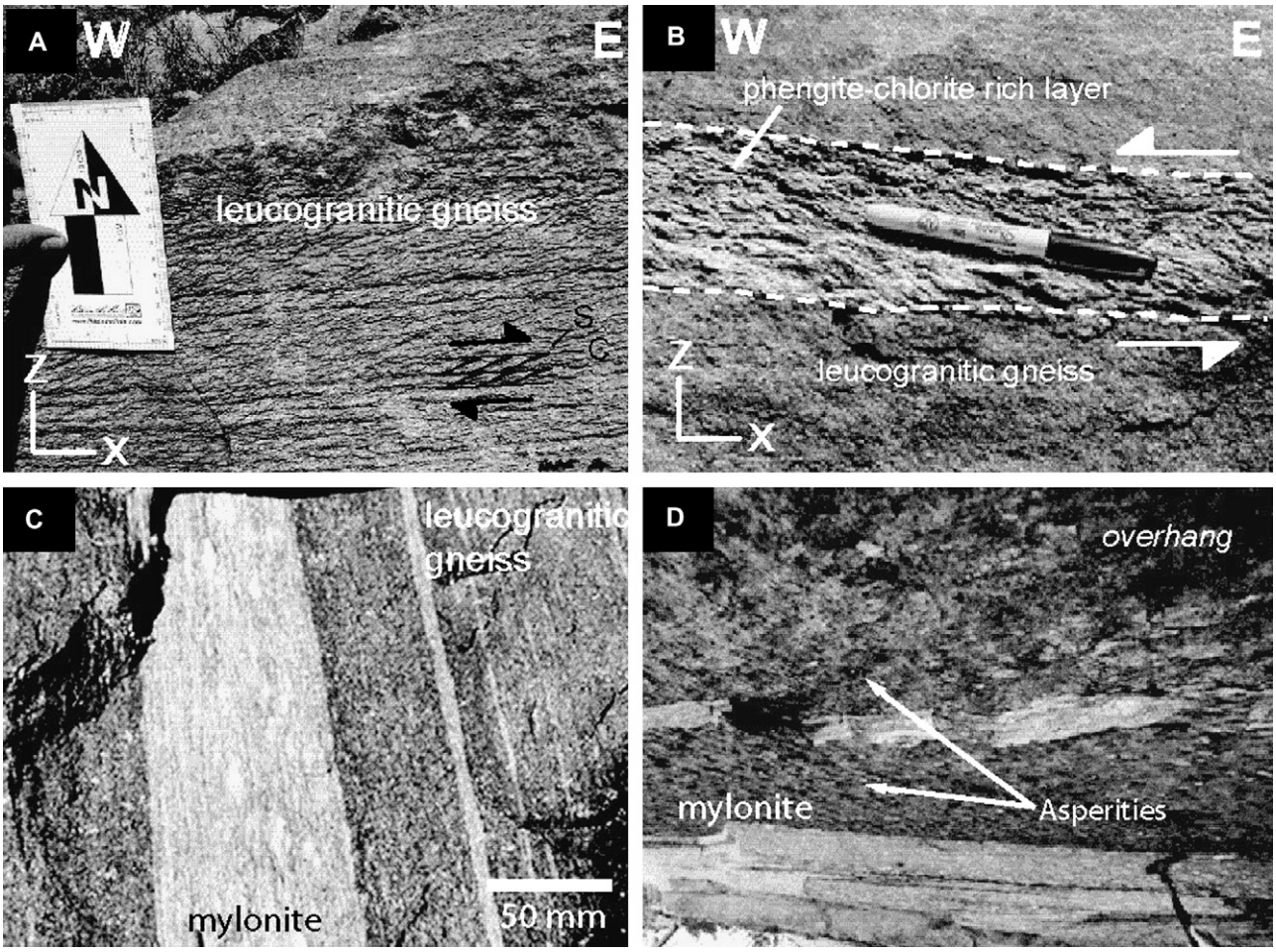

Fig. 4. Val Gilba gneisses and characteristic mesoscopic structures. (A) S-C structures indicating a top-to-east sense of shear; (B) phengite-chlorite rich layer conformable to compositional banding in host gneiss and parallel to mylonitic foliation in gneiss; (C) localized mylonitic zone and compositional banding in gneiss; (D) asperities within the foliation plane of the mylonitic gneiss.

spatially associated with any particular compositional band of the fine to medium grained gneisses.

The largest number of pseudotachylyte veins (>25) has been observed within the walls of small active quarries located near the base of a natural cliff in the fine to medium grained gneisses. The continuous quarrying operations provide an unparalleled opportunity to assess the extent of pseudotachylyte veins in 3-D. Pseudotachylyte veins occur also in outcrops outside the quarries but are far more difficult to identify.

A simplified nomenclature of pseudotachylyte geometry can be found in Ferré et al. (2005). Generation veins, the dominant geometric type, range from 1 to 10 mm in thickness and are parallel to the mylonitic foliation (Fig. 5). Thin veins are black and shiny (Fig. 5A,C) while larger veins are dark gray and have a dull luster (Fig. 5B). Paired sets of foliation-parallel generation veins, separated by a few tens of millimeters, are commonly observed in the Val Gilba area (Fig. 5C and E). Single injection veins are rare (Fig. 5D) whereas complex injection veins connecting two paired generation veins are more common (Fig. 5E). Pseudotachylyte reservoir veins are formed where a cataclastic domain in between two paired generation veins are invaded by friction melt (Fig. 5E). Vein networks have been observed in a few occurrences only (Fig. 5F).

Exposures in the quarries reveal the existence of several, mutually cross-cutting, generations of cataclasite, ultracataclasite and pseudotachylyte veins. Angular fragments of pseudotachylyte embedded in younger cataclasite attest to the occurrence of continued deformation after formation of post pseudotachylyte veins.

4. New microstructural observations on the pseudotachylytes and host rocks

Oriented rock specimens were cut perpendicular to foliation and parallel to lineation. Microstructures were observed in thin section (thickness of 20 μm only in pseudotachylytes) using a petrographic polarizing microscope. Additional observations were made using a Hitachi scanning electron microscope (SEM).

4.1. Val Gilba augen gneisses

These gneisses display a protomylonitic to mylonitic deformation characterized by the development of a strong lattice

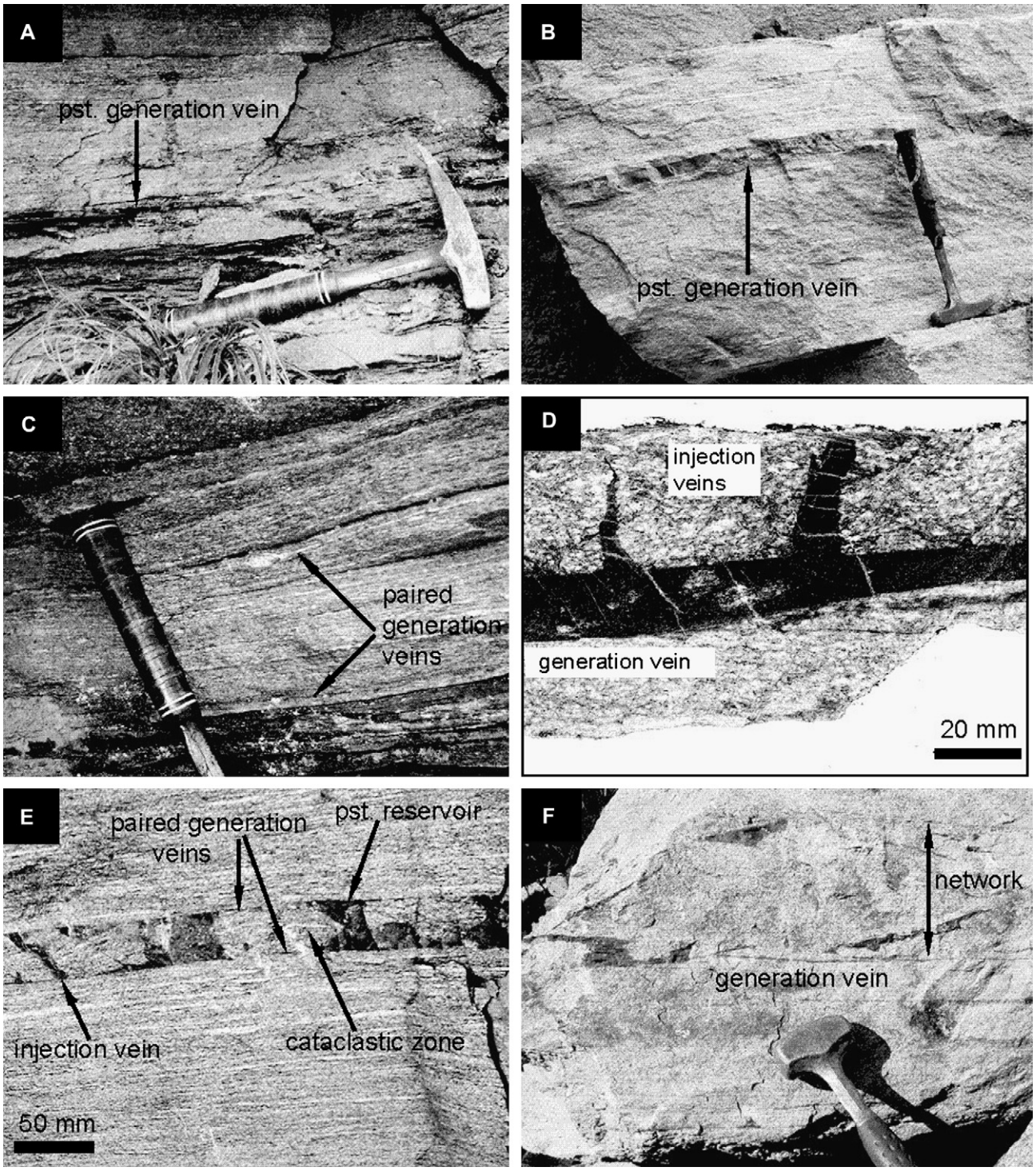

Fig. 5. Val Gilba pseudotachylyte veins and host mylonitic gneiss. (A) Simple generation vein parallel to foliation; (B) thick generation pseudotachylyte vein; (C) simple and paired generation veins; (D) generation vein and two injection veins; (E) paired generation veins, cataclastic zone and reservoir; (F) complex network in between two generation veins.

preferred orientation (LPO) and grain shape preferred orientation (SPO). Both of these are consistent with a top-to-east sense of shear. The augen gneisses consist of parallel bands and long lenses that tend to be monomineralic in composition. This is particularly the case for quartz that forms ribbons and phyllosilicates (phengite, green biotite) that form fairly continuous, albeit thin, layers.

Quartz occurs in two habits with different grain sizes. Coarse grains (100–500 μm) are found in ribbons about 1 mm thick, made of polygonal grain mosaic. These grains,

with an aspect ratio ranging from 1.5 to 4, display an individual elongation oblique to the ribbon. The strong LPO in these ribbons can be seen using a quartz λ auxiliary wedge. The coarse grained quartz exhibits sweeping undulose extinction and basal slip in the (c) <*a*> direction. Deformation bands or deformation lamellae were not observed. The edges of the coarse grained ribbons are straight and sharp, and in contact with either a band of fine grained quartz or a band of phyllosilicates. Finer grains (10–50 μm) form aggregates with polygonal to lobate contours. This type of finer quartz overprints coarse quartz ribbons and fills cracks in K-feldspar porphyroclasts.

K-feldspar forms large perthitic augen (up to 20 mm long) and a few smaller euhedral to anhedral grains (10–100 μm). Two subtypes of plagioclase augen can be distinguished in different samples: (i) stocky, subhedral grains with moderate to low anorthite content ($<An_{15}$) and a weak zonation; (ii) elongated, euhedral grains with higher anorthite content ($\approx An_{30}$–An_{40}), with Carlsbad twinning.

Other minerals include kinked and euhedral green biotite (both in the C and S planes) and phengite, tabular to grainy zoisite grains (<200 μm), titanite in small trails, small zircons ($\approx$30 μm), euhedral apatite, garnet and allanite. A few chlorite coated slickensides are observed in the quarries, within foliation planes and low-angle faults almost parallel to regional foliation. The relative timing of formation of these slickensides and pseudotachylyte veins could not be determined.

In the vicinity of pseudotachylyte veins (at less than 20 mm distance from contact), the microstructures of the host gneiss display significant changes: a larger number of biotite and phengite euhedral grains are kinked; the number of vein parallel fractures per unit area increases substantially and fractures become increasingly more parallel to the vein wall; a few thin veins filled with small (<10 μm) quartz angular clasts branch off the pseudotachylyte vein into the host rock at a shallow angle. Large grains of poikilitic garnet remain euhedral to subhedral and are not more fractured than away from the pseudotachylyte vein. Although the fracture density increases towards the pseudotachylyte vein, this does not lead to any significant decrease in grain size since displacement along the fractures seems limited. Mechanical twinning in plagioclase does not increase substantially towards the veins either.

4.2. Val Gilba fine to medium grained gneisses

These gneisses exhibit a microscopic mylonitic to ultramylonitic foliation characterized by a moderate SPO of major mineral phases and strong quartz LPO. This foliation overprints a banding defined by millimeter-thick bands of different compositions and grain sizes.

Quartz shows a unimodal grain size distribution ranging from 50 to 200 μm. Most grains exhibit sweeping undulose extinction and form a seriate to interlobate microstructure. Some grains display pinning microstructures indicative of substantial grain boundary migration. Quartz is practically free of any inclusions. A minor population of smaller grains ($\approx$50 μm) with lobate contours might indicate dynamic recrystallization.

K-feldspar occurs in general with the same size as quartz grains but, exceptionally, a few grains can be up to 0.6 mm in length. K-feldspar forms stocky grains with a distinctive microcline twin.

Plagioclase forms larger grains (up to 1 mm in length) characterized by both albite and Carlsbad twins, as well as mechanical (tapered) twins. Plagioclase does not show any substantial optical zoning and is characterized by intermediate anorthite content ($\approx An_{35}$–An_{50}). Plagioclase grains host numerous small inclusions of biotite, zircon and apatite.

Kinked green biotite (both in the C and S planes) and kinked and folded phengite form large grains (up to 3 mm long). Accessory minerals include euhedral zoisite, postdating phengite, euhedral titanite, allanite, garnet and rare anthophyllite.

4.3. Val Gilba pseudotachylytes

Microstructural observations were performed on thin sections prepared from 20 different hand specimens in which pseudotachylyte veins display thicknesses from 2 to 25 mm. These veins consist of a core of pseudotachylyte material surrounded by ultracataclasite. The proportion of pseudotachylyte material is highly variable along the veins. These veins are generally thinly zoned and range in color from brown to cream in PPL (Fig. 6A). Generation veins are locally separated from weakly deformed hot rock by a zone of cataclasite, 2–25 mm in width (Fig. 6B). Angular fragments of pseudotachylyte, several millimeters in length, occur in this cataclasite (Fig. 6A). A few of these fragments exhibit worn outlines, which suggests that some mechanical wear took place after pseudotachylyte solidification. Rounded polymineralic clasts containing both plagioclase and quartz are found in the pseudotachylyte (Fig. 6C).

The spherulitic microstructure of part of the vein constitutes compelling evidence for a glassy origin and hence melting. Under PPL, the spherulites appear as light colored disks of about 10–20 μm in diameter, made mostly of K-feldspar and quartz (10–20 μm). They are evenly distributed throughout the pseudotachylyte volume and form at an average spacing of about one diameter. The vein material is very fine grained and bears microstructural evidence, such as axiolitic microstructures, of devitrified glass.

Acicular feldspar microlites, ranging in size from 2 to 5 μm, exhibit a strong preferred orientation in an isotropic fine grained matrix (Fig. 6E). Several mechanisms could account for such orientation: (i) flow in the pseudotachylyte melt if microlites formed early; (ii) stress-controlled growth in solid state; (iii) compositional control over growth exerted by layers of different composition.

The recrystallized microcrystalline assemblage, both in the ultracataclasite and the pseudotachylitic devitrified glass, locally exhibits cleavage and S-C structures indicative of top-to-west sense of shear (Fig. 7). This fabric cuts through the limbs of isoclinal folds formed as the vein material was flowing.

The clast/matrix ratio in the pseudotachylyte vein varies considerably along and across veins. Two different matrices

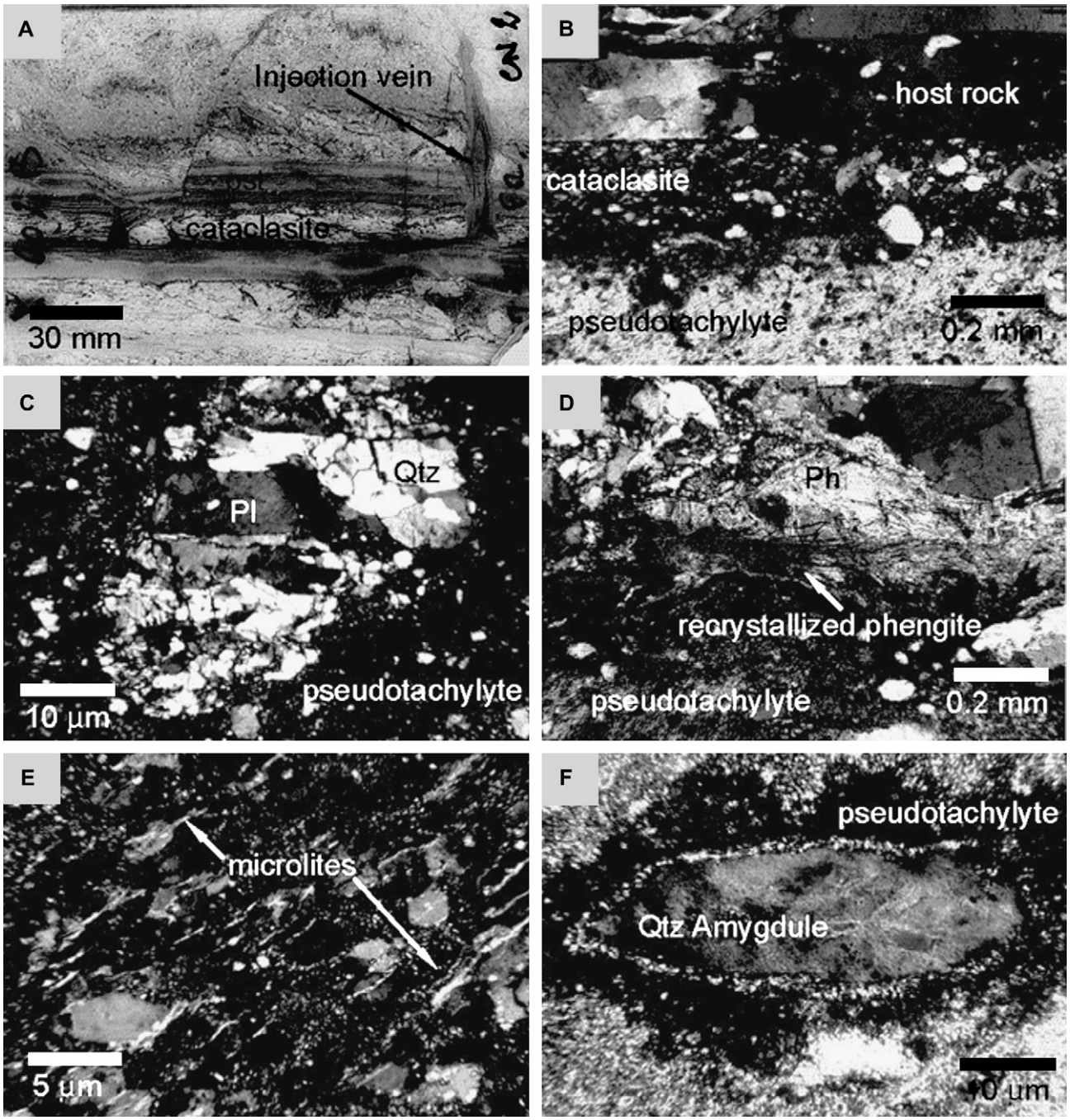

Fig. 6. Pseudotachylyte petrographic photomicrographs. (A) Two generations of cross-cutting pseudotachylyte veins; (B) pseudotachylyte locally separated from mylonitic gneiss by a cataclastic zone; (C) polymineralic fragment in a pseudotachylyte vein; (D) phengite and recrystallized phengite neoblasts in a pseudotachylyte; (E) feldspar microlites in a pseudotachylyte matrix; (F) quartz-filled amygdule in a pseudotachylyte.

have been observed: Type 1 is characterized by the abundance of small grain size (10–100 μm) white micas (Fig. 6D; phengite), possibly resulting from phengite selective melting and subsequent recrystallization during vein quenching. Type 2 is a mixture of isotropic and very fine-grained material interpreted as devitrified glass.

A flattened quartz-filled amygdule (50 μm long), representing vapor formed in the melt, was observed in the pseudotachylyte core of a vein (Fig. 6F). The lack of quartz corrosion microstructures suggests that melting temperatures were most likely below 1700 °C, as suggested elsewhere by Wenk et al. (2000).

5. Geochemistry of the pseudotachylyte veins and host rocks

A series of whole-rock major element X-ray fluorescence (XRF) analyses were performed on selected samples to

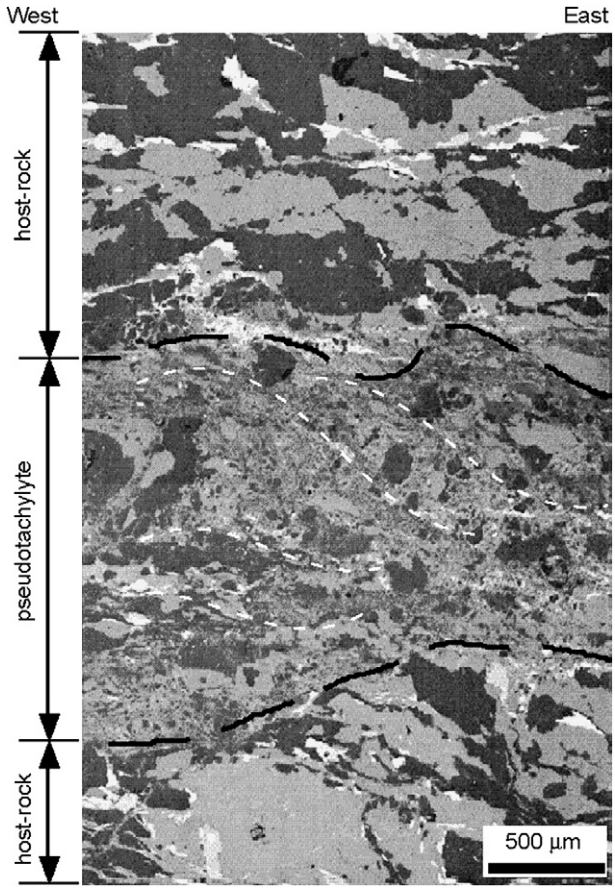

Fig. 7. Scanning electron microscopy image of a pseudotachylyte vein showing an S-C microstructure. Note the lack of cataclasite around the pseudotachylyte vein.

constrain the origin of friction melts. Similar studies applied to other pseudotachylytes localities have addressed two issues (Maddock, 1992; Magloughlin and Spray, 1992; Camacho et al., 1995; Lin and Shimamoto, 1998; O'Hara and Sharp, 2001; Moecher and Sharp, 2004; Warr and van der Pluijm, 2005): (i) whether melts were locally derived or transported along the veins and (ii) whether melting was complete (congruent) or selective (incongruent).

In our study, all specimens were fresh and collected from the Val Gilba active quarries. The analyzed material included (i) two specimens of the host gneiss collected about 50 mm away from the pseudotachylyte veins, (ii) three specimens of 10–20 mm thick pseudotachylyte veins, (iii) one specimen of a large phengite single crystal (30 mm diameter, 8 mm thick). The pseudotachylyte samples were selected to be free of visible gneiss fragments. The new geochemical data and that of Cosca et al. (2005) are given in Table 1.

The host gneiss has a fairly consistent composition at outcrop scale. In contrast, the pseudotachylyte veins show compositional variation for most oxides (Table 1). These variations, considering the very fine grain size of the vein rock, are not related to a lack of representativeness of the analyzed material. Such variations could be explained by variable clast/matrix ratios in the veins or by selective melting of specific phases. The isocon method, based on Gresens' equation (Gresens, 1967; Grant, 1986), has been applied to investigate the possibility that specific mineral phases melted preferentially. The six host gneiss compositions have been compared to the four pseudotachylyte compositions. The only assumption made in the isocon analysis was melting at constant mass. This analysis shows that various oxides display different mobilities during melting, in decreasing mobility: MgO, Fe_2O_3, MnO, K_2O, TiO_2, Al_2O_3, SiO_2, CaO, P_2O_5 and Na_2O (Table 1). The most important implication is that ferromagnesian minerals were most likely preferentially involved in the melting process. In addition, for most major oxides, pseudotachylytes have compositions intermediate between the host gneiss and a phengite-chlorite rich layer. This is particularly visible on a $(Fe_2O_3 + MgO + MnO)/Al_2O_3$ vs $(K_2O + CaO + Na_2O)/Al_2O_3$ diagram (Fig. 8). The phengite "monocrystal" (analysis #11 in Table 1), is deemed impure on the basis of its high FeO content and in comparison with phengite compositions determined by electron microprobe analysis elsewhere in the Dora Maira Massif (Di Vincenzo et al., 2006). The high FeO content could be accounted for by interbedded chlorite layers. These results suggest that the pseudotachylyte veins have a whole rock composition which is more phengitic-chloritic than the host gneiss. It should be noted that the pseudotachylyte veins do not host large grain of phengite, but that large clasts of feldspars and quartz are present.

6. Discussion

Geobarometric and geochronological data for ultra-high pressure (UHP) rock units suggests fast exhumation following the pressure peak of metamorphism, on the order of tens of millimeters per year (Hacker and Peacock, 1994; Ernst et al., 1997; Gebauer et al., 1997; Webb et al., 2001; Ratschbacher et al., 2003; Baldwin et al., 2004). Similar fast exhumation is recorded in the UHP gneisses of Norway (Labrousse et al., 2004), although these units were not extruded or emplaced on top of other low grade metamorphic units (Root et al., 2005). Such rapid exhumation implies high strain rates along crustal shear zones and faults. In turn, the combination of high strain rates and decreasing temperature should lead to cataclastic deformation and possibly to seismic activity. In the UHP units of the Val Gilba, seismic slip is documented by pseudotachylyte veins. However, the observed pseudotachylytes formed late in the exhumation process at ca. 20 Ma, i.e., following an initial period of extremely rapid exhumation between ca. 35 and 30 Ma then slowing from 30 to 20 Ma (Cosca et al., 2005). In the following discussion, the deformation regime and mode of formation of the Val Gilba pseudotachylytes will be discussed in an attempt to resolve this apparent paradox. In the following, the formation of the Val Gilba pseudotachylyte will be referred to as the main *seismic* event but this does not imply that seismic slip did not occur during earlier exhumation stages.

Table 1
XRF whole rock analyses of the Val Gilba gneisses, pseudotachylyte veins and phengitic rocks (weight %)

	Host gneiss						Pseudotachylyte vein				Phengite
	1	2	3	4	5	6	7	8	9	10	11
SiO_2	73.34	73.22	74.78	74.63	72.74	72.73	72.58	70.55	65.36	74.24	50.90
TiO_2	0.33	0.33	0.21	0.10	0.36	0.36	0.35	0.53	0.29	0.26	0.31
Al_2O_3	12.96	13.11	12.80	14.17	13.74	13.25	13.34	13.95	15.45	12.84	23.14
Fe_2O_3	2.13	2.28	2.39	1.15	2.52	3.37	2.51	4.05	3.74	2.61	8.10
MnO	0.03	0.04	0.04	0.03	0.05	0.06	0.04	0.07	0.06	0.05	0.10
MgO	0.34	0.35	0.07	0.24	0.43	0.23	0.71	0.76	2.26	0.35	1.40
CaO	0.76	0.85	0.75	0.54	0.97	1.24	0.71	0.88	0.40	0.77	0.17
Na_2O	3.33	3.38	3.18	3.28	3.38	2.86	1.86	0.44	0.23	2.75	0.14
K_2O	5.30	5.26	5.40	4.81	5.09	5.34	7.60	6.28	5.94	5.64	10.55
P_2O_5	0.10	0.10	0.04	0.23	0.13	0.09	0.11	0.16	0.03	0.06	0.00
$H_2O(-)$	0.30	0.36					0.04	0.24	0.99		0.35
$H_2O(+)$ CO_2	1.06	0.72					0.15	2.09	5.27		4.84
LOI			0.34	0.83	0.59	0.46				0.42	

All analyses are normalized to 100%. Analyses 1, 2, 7, 8, 9, 11, this study; 3–6, 10, Cosca et al. (2005).

6.1. Structures and microstructures related to pre-seismic deformation

Pre-seismic plastic strain in the host gneiss was examined several meters away from the pseudotachylyte veins and appears to be mostly penetrative albeit locally heterogeneous, mostly due to variations in composition of the Val Gilba gneiss.

The pre-seismic deformation regime in these gneisses was most likely in the semiductile regime, as suggested by the pervasive occurrence of S-C mylonitic fabrics that predate pseudotachylyte veins (Fig. 4). Indeed, S-C fabrics have been interpreted elsewhere as characteristic of deformation between the brittle and fully ductile regimes (e.g., Shimamoto, 1989; Nakamura and Nagahama, 2002). This regime, also referred to as frictional-viscous mylonitic flow (Handy et al., 1999), can be described by a composite flow law where the interconnected grains of the weak mineral (quartz) undergo a power law creep whereas the hard porphyroclasts (feldspars) deform by fracturing and frictional sliding. For granitic compositions comparable to the Val Gilba gneisses, the maximum strength reaches ca. 80 MPa (Handy et al., 1999).

The angle between the S and C plane [α] has been used to quantify shear strain [γ] in the case of simple shear deformation (Nicolas, 1987): $\gamma = 2 \times \cot 2\alpha$.

In the mylonitic gneisses, with an S-C angle of ca. 20°, the inferred shear strain γ is 2.4, while in the phengite layers, with an angle of ca. 30°, shear strain γ is 1.15. These shear strains are barely sufficient to account for the large aspect ratio of quartz ribbons (1:4 to 1:10) without a pure shear component from mylonitic deformation. This suggests that deformation was strongly partitioned during exhumation (Fig. 4C) and that the phengite layers as well as the mylonitic gneisses recorded only part of the total strain. Major strain-localizing structures, such as shear zones or faults, that would account for additional strain still remain to be identified.

The stability of green primary biotite in the C planes, as well as the quartz ribbon polygonal mosaic microstructure and the sweeping undulose extinction attest that the last substantial increments of deformation occurred at temperatures around 450–350 °C under moderate strain rates (ca. 10^{-13} to 10^{-14} s^{-1}) and modest differential stress (10–20 MPa) for the continental crust (Passchier and Trouw, 1996). Strain rates might have been slightly higher or deformation occurred at a lower temperature in the ultramylonitic bands (ca. 10^{-12} to 10^{-13} s^{-1}).

These microstructural observations indicate that the host gneiss recorded temperature-sensitive ductile flow during the

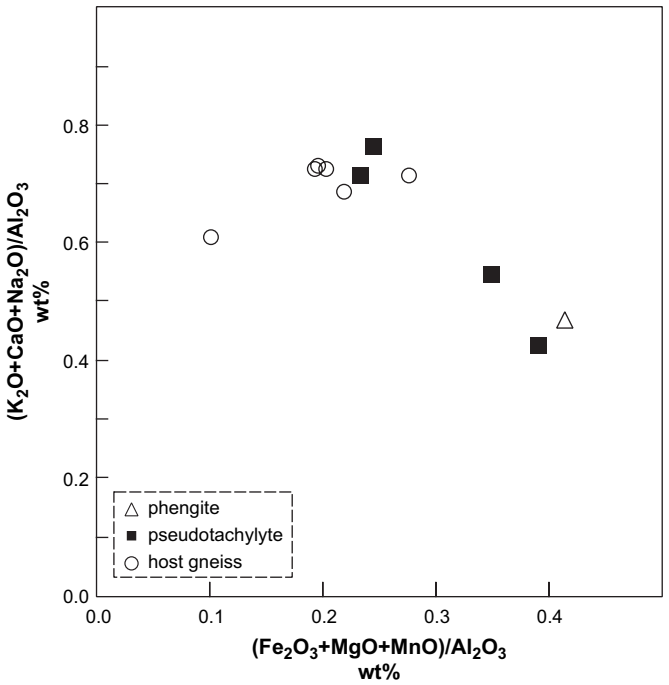

Fig. 8. Al_2O_3/CaO vs K_2O/Na_2O (wt%) whole rock compositions. The composition of the pseudotachylyte veins (filled squares) stands out with respect to that of the host gneiss (open circles), and tends towards a phengite-chlorite pole (open triangle).

exhumation process but did not record low temperature, high strain rate deformation prior to seismic slip.

6.2. Structures and microstructures related to coseismic deformation

At the macroscopic scale, the presence of abundant pseudotachylyte and injection veins in the Val Gilba gneisses is overwhelming evidence for coseismic deformation. However, unlike many other pseudotachylite localities, the Val Gilba veins are not closely related to faults or to substantial volumes of cataclasites or ultracataclasites (e.g., Lin, 1996; Fabbri et al., 2000; Wenk et al., 2000). Discrete faults and shear zones are most likely involved in the exhumation mechanism of the Dora Maira units but these are not anywhere close to the pseudotachylyte veins. This very peculiar situation could be explained by the fact that the pseudotachylyte host rock was already strongly anisotropic (mylonitic gneiss) as a result of continuous extensional shear in the ductile regime. The mylonitic foliation probably acted as a planar structural guide to focus deformation further. At the microscopic scale, in the immediate vicinity of the pseudotachylyte veins (<20 mm), the high strength mineral phases such as plagioclase and garnet do not exhibit any specific high stress microstructures. Garnet remains euhedral to subhedral, however plagioclase does show a slight increase in mechanical twinning. These observations contrast with those made by Lenze et al. (2005) in the Case Ramello locality of the Dora Maira Massif, where mechanical twinning in jadeite, cataclastic garnet and high density of twins in calcite suggests differential stresses up to 0.5 GPa. Similar observations have been made in the Sesia zone of the Western Alps (e.g., Küster and Stöckert, 1999; Trepmann and Stöckhert, 2003).

Although further microscopic investigations are required to adequately compare the Val Gilba and Case Ramello specimens, our preliminary results suggests that the Val Gilba gneisses did not experience very large stresses during exhumation. A possible explanation for these differences is that repeated seismic slip along the foliation plane of the Val Gilba gneisses might provide an efficient lubrication mechanism as suggested by recent experiments (Di Toro and Pennacchioni, 2004).

6.3. Microstructures related to post-seismic deformation

During and immediately after seismic slip occurred, frictional heat was transferred to the host gneiss. This process could, in principle, rheologically soften the host rock at a close distance from the veins, as described elsewhere by Passchier (1982).

In the Val Gilba rocks, microstructures indicative of post-seismic softening have not been observed. The efficiency of this process seems to have been limited due to the small average thickness of veins (5–10 mm) and, possibly, to a generally low post-seismic strain rate in the host gneiss. The pseudotachylytes exhibit S-C microstructures with top-to-west sense of shear (Cosca et al., 2005; this study). These microstructures formed, in the semiductile regime, after solidification of the pseudotachylyte melt, i.e., a few minutes to a few hours after the seismic event. A few asymmetric low-amplitude flow folds in the pseudotachylyte matrix attest that post-seismic displacement along the vein was limited.

6.4. Conditions of deformation

The confining pressure during formation of the pseudotachylyte veins can be constrained, by the presence of amygdules. Indeed, fluid inclusions, vugs, miarolitic cavities and amygdules form by exsolution of fluids from a magma due to a decrease in pressure during ascent. This phenomena can take at various depths but it becomes significantly more likely close to the surface, particularly at pressures less than 1 kbar (3–0.5 km). The size of these small fluid pockets increases as pressure decreases. By comparison with bubble size in hypovolcanic rocks (London, 1986), amygdules of 50 mm in length are likely to have formed under pressures <1 kbar. This is also supported by microstructural evidence of devitrification in the thick veins which indicates that the melts were quenched against a relatively cold host rock ($\leq$100 °C). The pseudotachylyte veins are dated around 20.1 $\pm$ 0.5 Ma (Cosca et al., 2005). This implies an average exhumation rate of 0.6–0.9 mm year^{-1} for the 30–20 Ma period.

The composition of pseudotachylyte veins has been used to infer the degree of melting. Wallace (1976) first suggested that fault pseudotachylytes along the Alpine Fault Zone of New Zealand are neither the product of selective melting of low-melting point phases nor the result of total melting. Small-scale variations across veins have recently been interpreted as resulting from in-situ crystal fractionation (Warr et al., 2005).

The composition of the Val Gilba pseudotachylyte is, in general, slightly more Al_2O_3, K_2O and Fe_2O_3 rich than the host rock (Fig. 8 and Table 1). This could be interpreted as (1) melting of a protolith that had a distinct composition from that of the host gneiss and/or (2) selective melting of specific mineral phases in the host gneiss. The persistence of quartz in the pseudotachylyte veins and the lack of quartz corrosion microstructures constrains the melting temperature to <1700 °C, as shown elsewhere by Wenk et al. (2000). It also shows that melting was incongruent since most quartz did not melt. The fact that the pseudotachylyte veins are parallel to the mylonitic foliation also suggests that pre-existing mechanical weaknesses in the host gneiss might have guided seismic slip. The phengite-chlorite rich zones, parallel to foliation, are likely to constitute a mechanically weak layer along which slip would be easier. Hence a difference in composition of the pseudotachylyte veins might reflect preferential melting resulting from seismic slip along phyllosilicate-rich layers.

The Val Gilba quarries expose several generations of pseudotachylyte veins suggesting multiple seismic events. The amount of displacement for each vein cannot easily be

determined by using offset markers because the veins developed parallel to the mylonitic foliation. However, a crude estimate can be made based on the empirical relationship between slip [d] and vein thickness [a] (Sibson, 1975).

$$d = 436a^2$$

In this model, which assumes that all work is dissipated by frictional heat, the volume of melt is proportional to displacement (both d and a are in meters and the relationship is not congruent with respect to units).

With representative thickness of generation veins of 0.5–1.0 mm (excluding zones of melt accumulation and ultracataclasite), the estimated slip is 1–4 m per vein. Such large slip would correspond to moderate to high magnitude earthquakes. Assuming an exhumation rate of 0.75 mm year^{-1} around 20 Ma and assuming that slip was entirely due to elastic response of the UHP units during exhumation, the periodicity of such earthquakes would have been on the order of 1–5 kyr.

The episodic vs steady-state slip behavior of faults is determined, to some extent, by their long term (10^5 year) slip rate (e.g., Chéry and Vernant, 2006). A high loading velocity is thought to result in low stress and constant slip rate whereas a low loading velocity should result in higher stresses and in the slip rate to vary cyclically between highs and lows (Chéry and Vernant, 2006). Hence, the 35–30 Ma exhumation history should be expected to be at a relatively constant slip rate while the 30–20 Ma should be characterized by episodic fault activity. In summary, a slower rate of exhumation may lead to seismic slip.

An alternative hypothesis would consider climatically driven rapid variation of the exhumation rate that would force the UHP rock units beyond their yield strength. This hypothesis will be discussed in the section on the Dora Maira exhumation model (Section 6.7).

6.5. Mylonite-pseudotachylyte association

The common occurrence of pseudotachylytes in mylonitic host rocks has for long been discussed because they each exemplify contrasted conditions of deformation (Hobbs et al., 1986; Fabbri et al., 2000; Lin et al., 2003). At the local scale, thermal softening in the immediate vicinity of a pseudotachylyte vein has been explained by the transfer of frictional heat from the vein into the host rock (Nicolas, 1987; Passchier, 1992). However, this effect is most likely insignificant because frictional heat is transferred relatively fast (on the order of minutes or hours) into the host rock. In addition, this effect would not account for the occurrence of a large volume of rocks undergoing mylonitic deformation and periodically cut by pseudotachylyte veins.

The model of frictional sliding instability proposed by Hobbs et al. (1986) provides an explanation (Note: A similar phenomenon causes brake shuttering in automobiles when the velocity goes to zero.) At constant normal stress, the deformation system can become unstable when the ratio of change in steady state frictional stress ($\delta\tau^{SS}$) to the change in sliding velocity (δV) becomes negative:

$$\delta\tau^{SS}/\delta V < 0$$

(velocity weakening occurs when $\delta V \leq 0$).

Finally, the formation of pseudotachylyte veins might have resulted from propagation of a failure surface from the upper crust schizosphere down into foliation-parallel surfaces in the plastosphere. This interpretation is consistent with the apparent lack of any brittle fault directly associated with the pseudotachylyte veins. A similar seismo-tectonic scenario has been proposed for the Sesia Zone, a zone situated in the same tectonic setting 100 km farther north along the Alpine arc (Trepmann and Stöckhert, 2003) and for the Dabie Shan pseudotachylytes (Lin et al., 2003).

6.6. Compositional banding and strain localization

Compositional banding in the host gneisses occurs at the scale of a few centimeters to a meter, mostly as bands of phyllosilicate rich quartz schist. The albite-rich bands in the leucocratic gneisses are surrounded by biotite selvages, a configuration that resembles that of a felsic leucosome surrounded by melanosome rims. This may indicate that initial exhumation may have started under partial melting conditions. The occurrence of quartz-rich bands adjacent to phyllosilicate-rich bands suggests that the phyllosilicate bands might form by a process of solid state metamorphic segregation in the host rock. Ultramylonite bands (grain size $\leq$50 μm, less than a few millimeters thick) display a high amount of micaceous matrix white mica) and compare well with other Alpine phengite-enriched ultramylonites such as those from the Argentera Massif (Corsini et al., 2004). As documented by Cosca et al. (2005), syn-exhumation plastic strain in the host gneiss is localized along the foliation plane which leads to the formation of mylonites and ultramylonites.

The occurrence of pseudotachylyte veins parallel to the foliation of mylonitic and ultramylonitic gneisses might be interpreted as extreme strain localization. If this were the case, one would anticipate finding pseudotachylytes within zones of ultracataclastic deformation. Indeed, the transition from ultramylonitization to frictional melting would require very large strain rates generally associated with ultracataclasis. The pseudotachylyte veins are not particularly located within ultracataclastic zones. In the Val Gilba thin sections that show the pseudotachylytes/host rock contact, the host is a mylonitic gneiss and not an ultracataclasite. In addition, the large polymineralic fragments incorporated into the pseudotachylyte vein are systematically from the coarse grained gneiss and not from an ultracataclastic protolith (Figs. 5E and 6C).

Although macroscopic and microscopic evidence argues against increasing strain localization leading to frictional melting, it is still possible that pseudotachylyte veins formed along a specific compositional boundary or within a specific compositional band of the host gneiss. This compositional control of seismic slip would explain the common occurrence of paired

pseudotachylyte veins separated by a network of pseudotachylyte and cataclasite (Fig. 5E).

The compositional control on the localization of pseudotachylyte veins is further supported by the whole vein major element composition. Pseudotachylyte veins exhibit higher contents of Al_2O_3, K_2O and Fe_2O_3 (Fig. 8 and Table 1) that are best explained by selective melting of a phengite-chlorite rich protolith. The presence of fine grained recrystallized phengite in the matrix of the pseudotachylyte veins also supports selective melting of phengite-chlorite rich layers (Fig. 9).

An explanation for the fact that the pseudotachylyte veins of the Val Gilba are not associated with any visible mesoscopic fault might be given by Francis (1972) who suggested that pseudotachylytes may be produced by reflection of shock waves in the rocks adjacent to the fault surface. This would also explain the distinct lack of pervasive cataclasis around the pseudotachylyte veins.

6.7. Implications for the exhumation model of the Dora Maira UHP units

The exhumation of the Dora Maira UHP units has been a subject of controversy regarding the extensional or compressional tectonic setting (Henry, 1990; Henry et al., 1993; Michard et al., 1993; Avigad et al., 2003). For example, Michard et al. (1993) favor extrusion tectonics for the main exhumation and restrict extension to the Mesoalpine gravitational collapse period. Our observations are restricted to the Val Gilba exposure and therefore do not pretend to offer a general solution to the problem. However, we note that the argument for or against a specific setting is generally based on observation of shear sense criteria. In the small area of the Val Gilba quarries, we document two apparently conflicting senses of shear: top-to-east in the mylonites and top-to-west in the phyllosilicate-rich layers. The two opposite senses of shear can be reconciled into one model where strain partitioning occurs as a result of a combination of simple shear and pure shear (Fig. 10). In this context the phyllosilicate-rich bands are interpreted as antithetic shear bands to the overall top-to-east mylonitic shear. This model is kinematically compatible with a significant flattening component in strain, in a similar manner to deformation in the western Norway HP-UHP terrains (Engvik and Andersen, 2000).

The exhumation of the Dora Maira UHP units can also be integrated in their regional setting. These rocks were formed at depth greater than 100 km at about 35 Ma (Gebauer et al., 1997). They had cooled down to ≈250 °C by 29.9 Ma (zircon fission track ages), which constrains their rate of exhumation to 20–30 mm year^{-1} in the 35–30 Ma period. This interpretation is consistent with the geochronological record in the neighboring Piedmont Tertiary Basin (Carrapa et al., 2003). Before ca. 38 Ma, $^{40}Ar/^{39}Ar$ geochronology on detrital white micas suggests a fast cooling and exhumation of the Western Alps including the Dora Maira Massif. The lower temperature ultramylonite bands of the Val Gilba are similar to the phengite-rich ultramylonites from the Argentera Massif formed around 27 Ma ($^{40}Ar/^{39}Ar$ on white mica, Corsini et al., 2003).

The upper Oligocene-Miocene evolution (30–10 Ma), in contrast, is characterized by slower cooling and exhumation. The only peak in the exhumation history recorded in this basin is in 20 Ma old, Aquitanian sediments that have a very short (almost 0) lag time, in turn implying extremely fast exhumation rates of the source (Carrapa, 2002).

Rapid climatic changes (in periods of time of 10^3–10^4 years) have been described elsewhere and were correlated with variations in seismic activity (e.g., Dadson et al., 2003;

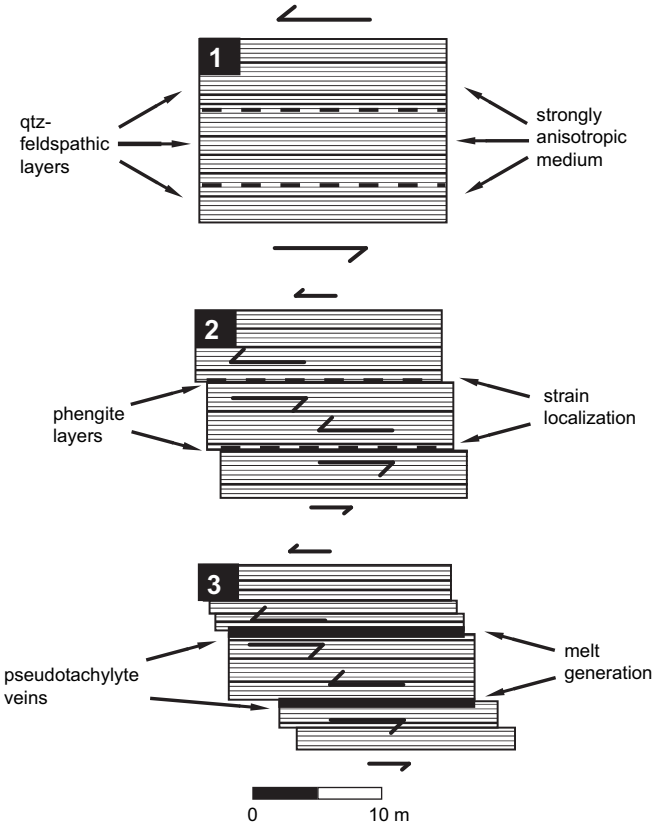

Fig. 9. Structural model illustrating preferential seismic slip along low-strength, phyllosilicate-rich, foliation-parallel surfaces.

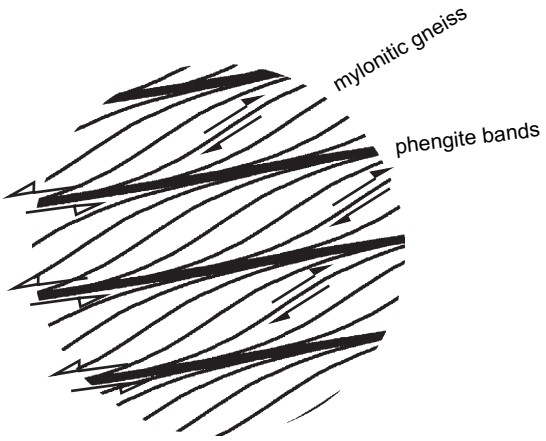

Fig. 10. S-C model for the opposite senses of shear observed in the mylonitic gneiss and phengite-chlorite rich bands.

Hetzel and Hampel, 2005; Chéry and Vernant, 2006). In the Dora Maira Massif, an increase in precipitation should lead to accelerated erosion and in turn faster unloading, which might cause faster exhumation. In this scenario, deformation that used to be accommodated by ductile processes at a given depth might no longer be possible and might involve brittle processes, thus leading to seismic rupture along foliation planes.

The laser-probe Ar-Ar technique used to date the pseudotachylytes is a proven method (e.g., Kelley et al., 1994; Sherlock and Hetzel, 2001; Kohút and Sherlock, 2003; Di Vincenzo et al., 2004). Therefore, the 20.1 ± 0.5 Ma age of the Val Gilba pseudotachylyte is considered reliable.

The Val Gilba pseudotachylytes cannot, at this stage, be related to the recent seismicity of the region. Indeed, differential exhumation in the Western Alps has been documented between blocks separated by tectonic discontinuities (Malusà et al., 2005). This might account for strain localization but would not explain the occurrence of pseudotachylyte veins in the Val Gilba since they are far from major discontinuities. Recent seismicity in the Dora Maira Massif, north of the Stura ''couloir'' (Giglia et al., 1996; Sue et al., 1999) is related to extension along normal faults.

7. Conclusion

In the Val Gilba area of the Dora Maira Massif, seismic slip is documented by pseudotachylyte veins cutting through UHP units. These veins formed late in the exhumation history, ca. 20 Ma, after a period of fast [35–30 Ma] and slow [30–20 Ma] exhumation. Pre-seismic deformation was in the semi-ductile regime as attested by the penetrative development of S-C structures throughout the pseudotachylyte host rock. The conditions are estimated to 450–350 °C, under strain rates of 10^{-13} to 10^{-14} s^{-1}, and differential stress of 10–20 MPa.

The Val Gilba pseudotachylytes, unlike numerous other examples (e.g., Fabbri et al., 2000; Wenk et al., 2000; Di Toro and Pennacchioni, 2004), are not associated with significant volumes of cataclasites or ultracataclasites. At the microscopic scale, close to the pseudotachylyte veins (<20 mm), the high strength mineral phases such as garnet and plagioclase, are free of high stress microstructural overprint. This contrasts with observations made elsewhere in the Dora Maira Massif. The difference might be explained by cyclic stress release along seismogenic melt-lubricated fault planes that formed along mica-rich horizons. These planes were most likely in a favorable orientation to release shear stress. Post-seismic deformation microstructures suggest that displacement along pseudotachylyte vein was limited after its formation.

The formation of pseudotachylyte veins is constrained to confining pressure of ≤1 kbar in a relatively cold host rock (≤100 °C). The bulk composition of the pseudotachylyte vein (clasts + matrix) is more Al_2O_3, K_2O, and Fe_2O_3 rich than the host rock and this is best explained by preferential seismic failure along phyllosilicate-rich, low mechanical strength planes. The slip events are estimated, using Sibson (1975)'s empirical formula, to have been 1–4 m per vein.

The episodic slip behavior of the fault plane can be explained by velocity weakening due to a low slip rate, when the ratio of steady state frictional stress ($\delta\tau^{SS}$) to the sliding velocity (δV) becomes negative. The nucleation of seismic failure is likely to have taken place in the schizosphere and propagated downwards into the plastosphere along the foliation plane.

The formation of pseudotachylyte veins parallel to the foliation of mylonitic and ultramylonitic gneisses does not result from extreme strain localization. The slip plane is compositionally determined by the presence of mechanically weak phyllosilicate-rich layers. This leads to the common development of paired pseudotachylyte veins (never triple).

The outcrop scale ductile sense of shear in the Val Gilba area are conjugate: top-to-east in the mylonites and top-to-west in the phyllosilicate-rich layers. This is interpreted as resulting from a combination of simple shear and pure shear.

At the regional scale, the upper Oligocene-Miocene evolution (30–10 Ma), is characterized by slow cooling and exhumation compared with the 50–30 Ma period. The only acceleration in exhumation rate recorded in detrital micas of neighboring basins is precisely at 20 Ma, when Aquitanian sediments reveal a very short lag time.

Acknowledgements

This research was funded by NSF Grant EAR-0228818. Our sincere thanks go to Renaud Caby for valuable discussion, to Carole Frima for assistance in the field and to Johanna Blake for whole rock analyses at UNM. One anonymous reviewer and Torgeir Andersen are sincerely acknowledged for their very constructive reviews which substantially improved the manuscript.

References

Agard, P., Monié, P., Jolivet, L., Goffe, B., 2002. Exhumation of the Schistes Lustrés complex; in situ laser probe 40Ar/39Ar constraints and implications for the Western Alps. Journal of Metamorphic Geology 20 (6), 599–618.

Amato, J.M., Johnson, C.M., Baumgartner, L.P., Beard, B.L., 1999. Rapid exhumation of the Zermatt-Saas ophiolite deduced from high-precision Sm-Nd and Rb-Sr geochronology. Earth and Planetary Science Letters 171, 425–438.

Andersen, T.B., Austrheim, H., 2006. Fossil earthquakes recorded by pseudotachylytes in mantle peridotite from the Alpine subduction complex of Corsica. Earth and Planetary Science Letters 242, 58–72.

Avigad, D., 1992. Exhumation of coesite-bearing rocks in the Dora Maira massif (western Alps, Italy). Geology 20, 947–950.

Avigad, D., Chopin, C., Goffe, B., Michard, A., 1993. Tectonic model for the evolution of the western Alps. Geology 21, 659–662.

Avigad, D., Chopin, C., Le Bayon, R., 2003. Thrusting and extension in the Southern Dora-Maira ultra-high-pressure massif (Western alps): view from below the coesite bearing units. The Journal of Geology 111, 57–70.

Baldwin, S.L., Monteleone, B.D., Webb, L.E., Fitzgerald, P.G., Grove, M., Hill, E.J., 2004. Pliocene eclogite exhumation at plate tectonic rates in eastern Papua New Guinea. Nature 431, 263–267.

Bruno, M., Compagnoni, R., Rubbo, M., 2001. The ultra-high pressure coronitic and pseudomorphous reactions in a metagranodiorite from the

Brossasco-Isasca Unit, Dora Maira Massif, western Italian Alps: a petrographic study and equilibrium thermodynamic modeling. Journal of Metamorphic Geology 19, 33–43.

Caby, R., 1996. Low-angle extrusion of high-pressure rocks and the balance between outward and inward displacements of Middle Penninic units in the western Alps. Eclogae Geologae Helvetiae 89, 229–267.

Caby, R., Ricou, L.E., 1999. East-directed low-angle extrusions and synconvergence exhumation of high-pressure units in the Western Alps. EUG 10 Strasbourg abstract 4 (1), 30.

Camacho, A., Vernon, R.H., Fitz Gerald, J.D., 1995. Large volumes of anhydrous pseudotachylyte in the Woodroffe Thrust, eastern Musgrave Ranges, Australia. Journal of Structural Geology 17 (3), 371–383.

Carrapa, B., 2002. Tectonic evolution of an active orogen as reflected by its sedimentary record, an integrated study of the Tertiary Piedmont Basin (Internal Western Alps, NW Italy). Unpublished PhD thesis, Vrije Universiteit of Amsterdam.

Carrapa, B., Wijbrans, J., Bertotti, G., 2003. Episodic exhumation in the Western Alps. Geology 31 (7), 601–604.

Chéry, J., Vernant, P., 2006. Lithospheric elasticity promotes episodic fault activity. Earth and Planetary Science Letters 243, 211–217.

Chopin, C., 1984. Coesite and pure pyrope in high-grade blueschists of the Western Alps: A first record and some consequences. Contributions to Mineralogy and Petrology 86, 107–118.

Chopin, C., Henry, C., Michard, A., 1991. Geology and petrology of the coesite bearing terrain, Dora Maira massif, Western Alps. European Journal of Mineralogy 3, 263–291.

Chopin, C., Schertl, H.P., 1999. The UHP Unit in the Dora Maira Massif, Western Alps. International Geological Reviews 41, 765–780.

Cliff, R.A., Barnicoat, A.C., Inger, S., 1998. Early Tertiary eclogite facies metamorphism in the Monviso Ophiolite. Journal of Metamorphic Geology 16 (3), 447–455.

Compagnoni, R., Hirajima, T., 2001. Superzoned garnets in the coesite-bearing Brossasco-Isasca Unit, Dora-Maira massif, Western Alps, and the origin of the whiteschists. Lithos 57, 219–236.

Corsini, M., Ruffet, G., Caby, R., 2004. Alpine and late-hercynian geochronological constraints in the Argentera Massif (Western Alps). Eclogae Geologae Helvetiae 97, 3–15.

Cosca, M.A., Caby, R., Bussy, F., 2005. Geochemistry and 40Ar-39Ar geochronology of pseudotachylyte associated with UHP whiteshists from the Dora Maira massif, Italy. Tectonophysics 402, 93–110.

Cowan, D., 1999. Do faults preserve a record of seismic slip? A field geologist's opinion. Journal of Structural Geology 21, 995–1001.

Dadson, S., Hovius, N., Chen, H., Dade, W.D., Hsieh, M.L., Willett, S.D., Hu, J.C., Horng, M.J., Chen, M.C., Stark, C.P., Lague, D., Lin, J.C., 2003. Links between erosion, runoff variability and seismicity in the Taiwan orogen. Nature 426, 648–651.

Di Toro, G., Pennacchioni, G., 2004. Superheated friction-induced melts in zoned pseudotachylites within the Adamello tonalites (Italian Southern Alps). Journal of Structural Geology 26, 1783–1801.

Di Toro, G., Pennacchioni, G., 2005. Fault plane processes and mesoscopic structure of a strong-type seismogenic fault in tonalites (Adamello batholith, Southern Alps). Tectonophysics 402, 55–80.

Di Vincenzo, G., Rocchi, S., Rossetti, F., Storti, F., 2004. 40Ar-39Ar dating of pseudotachylytes: the effect of clast-hosted extraneous argon in Cenozoic fault-generated friction melts from the West Antarctic Rift System. Earth and Planetary Science Letters 223, 349–364.

Di Vincenzo, G., Tonarini, S., Lombardo, B., Castelli, D., Ottolini, L., 2006. Comparison of 40Ar-39Ar and Rb-Sr data on phengites from the UHP Brossaco-Isasca Unit (Dora Maira Massif, Italy): implications for dating white mica. Journal of Petrology, 1–27, doi:10.1093/petrology/egl018.

Engvik, A.K., Andersen, T.B., 2000. The progressive evolution of Caledonian deformation fabrics under eclogite and amphibolite facies at Vårdalsneset. In: Journal of Metamorphic Geology, 18. Western Gneiss Region, Norway. 241–257.

Ernst, W.G., Maruyama, S., Wallis, S., 1997. Buoyancy-driven, rapid exhumation of ultrahigh-pressure metamorphosed continental crust. Proceedings of the National Academy of Science USA 94, 9532–9537.

Fabbri, O., Lin, A., Tokushige, H., 2000. Coeval formation of cataclasite and pseudotachylite in a Miocene forearc granodiorite, southern Kyushu, Japan. Journal of Structural Geology 22, 1015–1025.

Ferré, E.C., Zechmeister, M., Geissman, J., MathanaSekaran, N., Kocak, K., 2005. The origin of high magnetic remanence in fault pseudotachylites: theoretical considerations and implications for co-seismic electrical currents. Tectonophysics 402, 125–139.

Francis, P.W., 1972. The pseudotachylyte problem. Comments on Earth Sciences: Geophysics 3 (2), 35–53.

Gebauer, D., Schertl, H.P., Brix, M., Schreyer, W., 1997. 35 Ma old ultrahigh-pressure metamorphism and evidence for very rapid exhumation of the Dora Maira Massif, Western Alps. Lithos 41 (1-3), 5–24.

Gebauer, D., 1999. Alpine geochronology of the Central and Western Alps: new constraints for a complex geodynamic evolution. Schweizerische Mineralogische und Petrographische Mitteilungen 79, 191–208.

Giglia, G., Capponi, G., Crispini, L., Piazza, M., 1996. Dynamics and seismotectonics of the West-Alpine arc. Tectonophysics 267, 143–175.

Grant, J.A., 1986. The isocon diagram - a simple solution to Gresens' equation for metasomatic alteration. Economic Geology 81, 1976–1982.

Gresens, R.L., 1967. Composition - volume relationships of metasomatism. Chemical Geology 2, 47–65.

Hacker, B.R., Peacock, S.M., 1994. Creation, preservation, and exhumation of ultrahigh pressure metamorphic rocks. In: Coleman, R.G., Wang, X. (Eds.), Ultrahigh Pressure Metamorphism. Cambridge University Press, Cambridge, pp. 159–181.

Handy, M.R., Wissing, S.B., Streit, L.E., 1999. Frictional-viscous flow in mylonite with varied bimineralic composition and its effect on lithospheric strength. Tectonophysics 303, 175–191.

Henry, C., 1990. L'unité à coésite du massif Dora Maira dans son cadre pétrologique et structural (Alpes occidentales, Italie). Université de Paris VI.

Henry, C., Michard, C., Chopin, C., 1993. Geometry and structural evolution of ultra-high-pressure and high pressure rocks from the Dora-Maira massif, Western Alps, Italy. Journal of Structural Geology 15 (8), 965–981.

Hermann, J., 2003. Experimental evidence for diamond-facies metamorphism in the Dora-Maira massif. Lithos 70, 163–182.

Hetzel, R., Hampel, A., 2005. Slip rate variations on normal faults during glacial-interglacial changes in surface loads. Nature 435, 81–84.

Hobbs, B.E., Ord, A., Teyssier, C., 1986. Earthquakes in the ductile regime. Pure and Applied Geophysics 124 (1/2), 309–336.

Kelley, S.P., Reddy, S.M., Maddock, R., 1994. Laser-probe 40Ar-39Ar investigation of a pseudotachylyte and its host rock from the Outer Isles thrust, Scotland. Geology 22 (5), 443–446.

Koch, N., Masch, L., 1992. Formation of Alpine mylonites and pseudotachylites at the base of the Silvretta nappe, Eastern Alps. Tectonophysics 204, 289–306.

Kohút, M., Sherlock, S., 2003. Laser microprobe ^{40}Ar-^{39}Ar analysis of pseudotachylyte and host-rocks from the Tatra Mountains, Slovakia: evidence for late Palaeogene seismic/tectonic activity. Terra Nova 15 (6), 417–424.

Küster, M., Stöckert, B., 1999. High differential stress and sublithostatic pore fluid pressure in the ductile regime – microstructural evidence for short-term post seismic creep in the Sesia Zone, Western Alps. Tectonophysics 303, 263–277.

Labrousse, L., Jolivet, L., Andersen, T.B., Agard, P., Hébert, R., Maluski, H., Schärer, U., 2004. Pressure-temperature-time-deformation history of the exhumation of ultra-high pressure rocks in the Western Gneiss region. In: Special paper, 380. Geological Society of America, Norway. 155–183.

Lacassin, R., Mattauer, M., 1985. Kilometer-scale sheath folds at Mattmark and the implications for transport direction in the Alps. Nature 315 (6022), 739–742.

Lapen, T.J., Johnson, C.M., Baumgartner, L.P., Mahlen, N.J., Beard, B.L., Amato, J.M., 2003. Burial rates during prograde metamorphism of an ultra-high-pressure terrane; an example from Lago di Cignana, Western Alps, Italy. Earth and Planetary Science Letters 215, 57–72.

Lenze, A., Stöckhert, B., Wirth, R., 2005. Grain scale deformation in ultra-high-pressure metamorphic rocks – an indicator of rapid phase transformation. Earth and Planetary Science Letters 229, 217–230.

Lin, A., 1994. Glassy pseudotachylyte veins from the Fuyun fault zone, northwest China. Journal of Structural Geology 16 (1), 71–83.

Lin, A., 1996. Injection veins of crushing-originated pseudotachylite and fault gouge formed during seismic faulting. Engineering Geology 43, 213–224.

Lin, A., Shimamoto, T., 1998. Selective melting process as inferred from experimentally generated pseudotachylytes. Journal of Asian Earth Sciences 16 (5-6), 533–545.

Lin, A., Sun, Z., Yang, Z., 2003. Multiple generations of pseudotachylyte in the brittle to ductile regimes, Qinling-Dabie Shan ultrahigh-pressure metamorphic complex, central China. The Island Arc 12, 440–452.

London, D., 1986. Formation of tormaline-rich gem pockets in miarolitic pegmatites. American Mineralogist 71, 396–405.

Lund, M.G., Austrheim, H., 2003. High-pressure metamorphism and deep-crustal seismicity: evidence from contemporaneous formation of pseudotachylytes and eclogite facies coronas. Tectonophysics 372, 59–83.

Maddock, R., 1992. Effects of lithology, cataclasis and melting on the composition of fault-generated pseudotachylytes in Lewisian gneiss, Scotland. Tectonophysics 204, 261–278.

Magloughlin, J.F., 1989. The nature and significance of pseudotachylite from the Nason terrane, North Cascade Mountains, Washington. Journal of Structural Geology 11, 907–917.

Magloughlin, J.F., Spray, J.G., 1992. Frictional melting processes and products in geological materials. Tectonophysics 204, 197–206.

Malusà, M.G., Polino, R., Zattin, M., Bigazzi, G., Martin, S., Piana, F., 2005. Miocene to Present differential exhumation in the Western Alps: insights from fission track thermochronology. Tectonics 24 (TC3004), doi:10.1029/2004TC001782.

Masch, L., 1970. Die pseudotachylite der Silvretta. Eine untersuchung ihrer deformation und aufschmelzung. Unpublished PhD thesis, Munich.

McKenzie, D., Brune, J.N., 1972. Melting on fault planes during large earthquakes. Geophysical Journal of the Royal Astronomical Society 29, 65–78.

Messiga, B., Kienast, J.R., Rebay, G., Riccardi, M.P., Tribuzio, R., 1999. Cr-rich magnesiochloritoid eclogites from the Monviso ophiolites (Western Alps, Italy). Journal of Metamorphic Geology 17 (3), 287–299.

Michard, A., Chopin, C., Henry, C., 1993. Compression versus extension in the exhumation of the Dora-Maira coesite-bearing unit, Western Alps, Italy. Tectonophysics 221, 173–193.

Moecher, D.P., Sharp, Z.D., 2004. Stable isotope and chemical systematics of pseudotachylites and wall rock, Homestake shear zone, Colorado, USA: meteoric fluid or rock buffered conditions during coseismic fusion. Journal of Geophysical Research 109, 1–11.

Monié, P., Philippot, P., 1989. Mise en évidence de l'age éocene moyen du métamorphisme de haute-pression dans la nappe ophiolitique du Monviso (Alpes occidentales) par la méthode ^{40}Ar-^{39}Ar. Comptes Rendus de l'Académie des Sciences, Série 2, Mécanique, Physique, Chimie, Sciences de l'Univers. Sciences de la Terre 309 (2), 245–251.

Montési, L.G.J., Hirth, G., 2003. Grain size evolution and the rheology of ductile shear zones: from laboratory experiments to postseismic creep. Earth and Planetary Science Letters 211, 97–110.

Nakamura, N., Nagahama, H., 2002. Tribochemical wearing in S-C mylonites and its implication to lithosphere stress level. Earth Planets and Space 54, 1103–1108.

Nicolas, A., 1987. Principles of Rock Deformation. Reidel, Dordrecht.

Obata, M., Karato, S., 1995. Ultramafic pseudotachylite from the Balmuccia peridotite, Ivrea-Verbano zone, northern Italy. Tectonophysics 242, 313–328.

O'Hara, K.D., Sharp, Z.D., 2001. Chemical and oxygen isotope composition of natural and artificial pseudotachylyte: role of water during frictional fusion. Earth and Planetary Science Letters 184, 393–406.

Passchier, C.W., 1982. Pseudotachylite and the development of ultramylonite bands in the Saint-Barthélemy Massif, French Pyrenees. Journal of Structural Geology 4, 69–79.

Passchier, C.W., Trouw, R.A.J., 1996. Microtectonics. Springer-Verlag, Berlin, 325 pp.

Philippot, P., 1990. Opposite vergence of nappes and crustal extension in the French-Italian western Alps. Tectonics 9, 1143–1164.

Ratschbacher, L., Hacker, B.R., Calvert, A., Webb, L.E., Grimmer, J.C., McWilliams, M.O., Ireland, T., Dong, S., Hu, J., 2003. Tectonics of the Qinling (Central China): tectonostratigraphy, geochronology, and deformation history. Tectonophysics 366, 1–53.

Root, D.B., Hacker, B.R., Gans, P.B., Ducea, M.N., Eide, E.A., Mosenfelder, J.L., 2005. Discrete ultrahigh-pressure domains in the Western Gneiss Region, Norway: implications for formation and exhumation. Journal of Metamorphic Geology 23 (1), 45–61.

Rubatto, D., Gebauer, D., Fanning, M., 1998. Jurassic formation and Eocene subduction of the Zermatt-Saas-Fee ophiolites; implications for the geodynamic evolution of the Central and Western Alps. Contribution to Mineralogy and Petrology 132 (3), 269–287.

Rubatto, D., Hermann, J., 2004. Exhumation as fast as subduction? Geology 29, 3–6.

Schertl, H.P., Schreyer, W., Chopin, C., 1991. The pyrope-coesite rocks and their country rocks at Parigi, Dora Maira massif, Western Alps: detailed petrography, mineral chemistry and PT-path. Contributions to Mineralogy and Petrology 108, 1–21.

Sharp, Z.D., Essene, E.J., Hunziker, J.C., 1993. Stable isotope geochemistry and phase equilibria of coesite-whiteschists, Dora Maira Massif, Western Alps. Contribution to Mineralogy and Petrology 114, 1–12.

Sherlock, S.C., Hetzel, R., 2001. A laser-probe ^{40}Ar-^{39}Ar study of pseudotachylite from the Tambach Fault Zone, Kenya: direct isotopic dating of brittle faults. Journal of Structural Geology 23, 33–44.

Shimamoto, T., 1989. The origin of S-C mylonites and a new fault-zone model. Journal of Structural Geology 11, 51–64.

Sibson, R.H., 1975. Generation of pseudotachylite by ancient seismic faulting. Geophysical Journal of the Royal Astronomical Society 43, 775–794.

Sue, C., Thouvenot, F., Fréchet, J., Tricart, P., 1999. Earthquake analysis reveals widespread extension in the core of the Western Alps. Journal of Geophysical Research: Solid Earth 104, 25611–25622.

Techmer, K.S., Ahrendt, H., Weber, K., 1992. The development of pseudotachylyte in the Ivrea-Verbano Zone of the Italian Alps. Tectonophysics 204, 307–322.

Trepmann, C.A., Stöckhert, B., 2003. Quartz microstructures developed during non-steady state plastic flow at rapidly decaying stress and strain rate. Journal of Structural Geology 25, 2035–2051.

Wallace, R.C., 1976. Partial fusion along the Alpine Fault Zone, New Zealand. Geological Society of America Bulletin 87, 1225–1228.

Warr, L.N., van der Pluijm, B.A., 2005. Crystal fractionation in the friction melts of seismic faults (Alpine Fault, New Zealand). Tectonophysics 402, 111–124.

Webb, L.E., Ratschbacher, L., Hacker, B.R., Dong, S., 2001. Kinematics of exhumation of high- and ultrahigh-pressure rocks in the Hong'an and Tongbai Shan of the Qinling-Dabie collisional orogen, eastern China. In: Hendrix, M.S., Davis, G.A. (Eds.), Geological Society of America Memoir No. 194. Paleozoic and Mesozoic Tectonic Evolution of Central Asia: From Continental Assembly to Intracontinental Deformation. Geological Society of America, Boulder, CO, pp. 231–246.

Wenk, H.R., Johnson, L.R., Ratschbacher, L., 2000. Pseudotachylites in the Eastern Peninsular Ranges of California. Tectonophysics 321, 253–277.

Wheeler, J., 1991. Structural evolution of a subducted continental sliver: the northern Dora Maira massif, Italian Alps. Journal of the Geological Society of London 148, 1101–1114.